Calix[4]arene-Filled Poly dimethylsiloxane (PDMS) Membranes for the Pervaporative Removal of Benzene from Dilute Aqueous Solution

Liang Liu,[1,2] Zhongyi Jiang,[1,2] Fusheng Pan[1]

[1]*School of Chemical Engineering and Technology, Tianjin University, Tianjin 300072, People's Republic of China*
[2]*State Key Laboratory of Functional Polymer Materials for Adsorption and Separation, Nankai University, Tianjin 300071, People's Republic of China*

Received 25 January 2005; accepted 5 September 2005
DOI 10.1002/app.23468
Published online 5 April 2006 in Wiley InterScience (www.interscience.wiley.com).

ABSTRACT: In this article, *tert*-butylcalix [4]arene (CA)-filled poly dimethylsiloxane (PDMS) membranes (CA-*f*-PDMS) were prepared for pervaporative removal of benzene from aqueous solution. In comparison with unfilled PDMS membrane, CA-*f*-PDMS membranes showed higher permselectivity towards benzene due to the inclusion interaction between benzene and CA. The separation factor increased from 3275 to 5604 when the CA content varies from 0 to 3 wt % in the PDMS membrane. On the other hand, the normalized permeation rate of benzene (NPR_b) decreased with the increase of the degree of crystallization of the membranes due to the crystallinity of CA. The membrane with 1 wt % CA content had the highest degree of crystallization and thus the lowest NPR_b, whereas the membrane with 3 wt % CA content was the opposite. Furthermore, the addition of CA increased the elastic modulus of membranes slightly. © 2006 Wiley Periodicals, Inc. J Appl Polym Sci 101: 90–100, 2006

Key words: calix [4]arene; PDMS; filled membrane; pervaporation; crystallization

INTRODUCTION

For the removal of volatile organic compounds (VOCs) from their dilute aqueous solutions, separation technologies such as carbon adsorption and air stripping are widely adopted at present. Pervaporation has been proved as an attractive and potentially cost-competitive candidate by many researches.[1–10] Unlike air stripping, pervaporation releases negligible amount of VOCs to the outside air. Unlike activated carbon, the separating medium does not require frequent replacement and disposal. Among common organophilic polymers, poly dimethylsiloxane (PDMS) has been proven to have the best performance in the pervaporative removal of volatile organic compounds (VOCs) from their dilute aqueous solutions by many researches.[11–14] PDMS exhibits relatively high permeability and is ideal for VOCs to pass through because of the flexible molecule chains and high-free volume. However, there is still much more room for the improvement of PDMS membrane performances, which are evaluated by permeability, permselectivity, and mechanical strength, etc. To serve this purpose, several approaches have been employed, for example, grafting,[7,15,16] blocking,[17] crosslinking,[18,19] filling,[11] and surface modification.[20] As a simple and effective way, the method of adding hydrophobic and organophilic filler into the matrix of PDMS membrane has attracted considerable research interest.[21–24] It is well known that the π-rich calixarene cavity is suitable for the inclusion of neutral guest of complementary size. Therefore, the incorporation of calixarene with adsorptive capability towards VOCs into PDMS membrane may potentially increase the permselectivity and/or permeability remarkably. Uragami et al.[25] has investigated the effect of the addition of *tert*-butylcalix [4] arene (CA) to PMMA-*b*-PDMS membrane for the removal of benzene from dilute aqueous solution. The experimental results indicated that the addition of CA to PMMA-*b*-PDMS membrane increased the separation factor from 1800 to 2300 and normalized the permeation rate from 7 to 13 (10^{-6}kgm/m^2 h). However, the inherent glassy characteristics of PMMA and the existence of microphase separation in PMMA-*b*-PDMS membrane may limit the permselectivity and permeability to some extent. We thus envisaged that the permselectivity and permeability of CA-filled pure

Correspondence to: Z. Jiang (zhyjiang@tju.edu.cn).
Contract grant sponsor: Cross-Century Talent Raising Program of Ministry of Education of China.
Contract grant sponsor: Sinopec Research Program; contract grant number: X500003.
Contract grant sponsor: Key project of Ministry of Education of China.

PDMS membranes may be higher than those CA-filled PMMA-*b*-PDMS membranes.

In this article, CA-*f*-PDMS membranes were prepared by adding different amount of CA into pure PDMS membranes for the pervaporative removal of benzene from its dilute aqueous solution. The effects of filling amount and crystallization behavior of CA on the permselectivity and permeability were also investigated.

Mass transfer through the membrane

Pervaporation mass transport is most often described according to the so-called solution–diffusion model, considered as a cornerstone in this field.[26] The permeation process can be divided into three steps: (1) sorption into the membrane at the upstream, feed side, (2) diffusion through the membrane, and (3) desorption or vaporization at the downstream, permeate side.

Furthermore, there are also two assumptions in the model developed here. (1) Mass transport through the membrane is usually considered to be rate-determining. This assumption implies that surface processes such as sorption at the feed-membrane interface and vapor desorption at the membrane-permeate interface are fast compared with diffusion processes through the membrane. (2) The interfaces of the membrane are in equilibrium with the upstream and downstream phases. This assumption means that the chemical potentials of component i in the upstream and downstream phases are equal to the chemical potential of component i just inside the membrane.

According to Fick's law, the permeation rate (PR_i) (kg/m^2 h) of component i in a polymer membrane can be defined as

$$PR_i = -D_i \frac{dC_i}{dl} \tag{1}$$

or

$$PR_i = D_i \frac{C_{if} - C_{ip}}{l} \tag{2}$$

where D_i is the diffusion coefficient, which depends strongly on the properties of components and the microstructure of the membrane; l is the thickness of the membrane; C_{if},C_{ip} are the component concentrations in the feed side and permeate side of the membrane.

Because of the extremely low pressure at the downstream, C_{ip} is usually considered to be zero. To eliminate the effect of the membrane thickness, the normalized permeation rate (*NPR*), the product of l and PR, is introduced. Then the eq. (2) may be expressed in a simplified form.

$$NPR_i = C_i \times D_i \tag{3}$$

where C_i is the component concentration in the feed side of the membrane.

To describe the permeability of the component in heterogeneous polymer systems, several models have been established. Among them, Maxwell model, which was proposed for analyzing the specific resistance of a continuum filled with dilute suspension of spheres, was frequently adopted. In this article, *NPR* can be described by eq.(4):

$$\frac{NPR_i^{fp}}{NPR_i^{p}} = 1 + 3\phi_f\left(\frac{\beta + 2}{\beta - 1} - \phi_f\right)^{-1} \text{ and } \beta = \frac{NPR_i^{f}}{NPR_i^{p}} \tag{4}$$

where the superscript *fp*, *p*, and *f* represent the filled polymer, the polymer, and the filler, respectively, and Φ_f is the volume fraction of the filler. When the filler is impermeable, $NPR_i^f = 0$ and eq. (4) can be simplified into eq. (5):

$$NPR_i^{fp} = NPR_i^{p}\left(\frac{1 - \phi_f}{1 + \frac{\phi_f}{2}}\right) \tag{5}$$

Equation (5) has been used successfully to describe the effect of filler content on permeability in a variety of filled polymers.[27,28] When eqs. (3) and (5) are combined, NPR_i^{fp} can be expressed by eq. (6):

$$NPR_i^{fp} = C_i^{fp} \times D_i^{fp} = C_i^{p} \times D_i^{p}\left(\frac{1 - \phi_f}{1 + \frac{\phi_f}{2}}\right) \tag{6}$$

It is often assumed that in the eq. (6), C_i^{fp} is equal to C_i^p. In fact, when the filler has a considerable adsorption capacity towards the permeating components, C_i^{fp} is usually higher than C_i^p and eq. (6) needs to be further modified as eq. (7):

$$NPR_i^{fp} = C_i^{fp} \times D_i^{p}\left(\frac{1 - \phi_f}{1 + \frac{\phi_f}{2}}\right) = C_i^{fp} \times \frac{C_i^{p}}{C_i^{p}} \times D_i^{p}\left(\frac{1 - \phi_f}{1 + \frac{\phi_f}{2}}\right) = \frac{C_i^{fp}}{C_i^{p}} \times NPR_i^{p}\left(\frac{1 - \phi_f}{1 + \frac{\phi_f}{2}}\right) \tag{7}$$

Furthermore, when the filler is of crystallinity, the diffusion behavior of the permeating components in the membrane will alter more or less. To reflect the effect of crystallization, the parameter D_c, which denotes the degree of crystallization, is introduced and

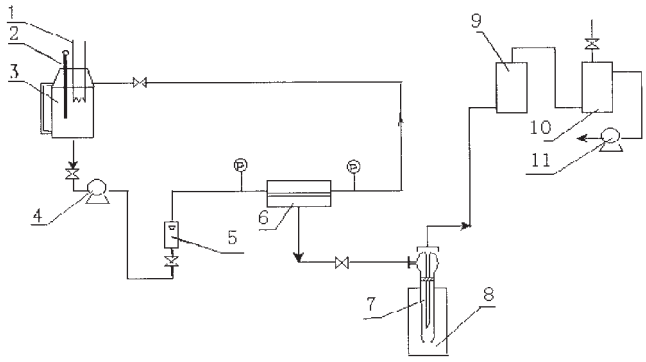

Figure 1 Schematic diagram of the PV experimental equipment. 1-Heater; 2-Thermocouple; 3-Feed container; 4-Feed circulator; 5-Flow meter; 6-Membrane cell; 7-Cold trap; 8-Liquid nitrogen; 9-Desiccator; 10-Buffer; and 11-Vacuum pump.

the factor $\dfrac{1-\phi_f}{1+\dfrac{\phi_f}{2}}$ in eq. (7) is substituted by $\left(\dfrac{\gamma \times D_c^p}{\gamma \times D_c^p + D_c^f}\right)$, where D_c^p is the D_c value of the polymer determined by the ratio of the minicrystal area to the total area in the XRD pattern and D_c^f is the D_c value of the filler in the polymer determined by the ratio of the filler's crystal area to the total area in the XRD patterns, as shown in Figure 11. A correction factor γ is introduced to eliminate the disturbance from the amorphous part of polymer.

Considering all the above-mentioned factors, a new model is tentatively proposed in hopes of fitting the permeability of the component in the polymer filled with crystal adsorbent more accurately (eq. (8)):

$$NPR_i^{fp} = NPR_i^p \times \frac{C_i^{fp}}{C_i^p} \times \left(\frac{\gamma \times D_c^p}{\gamma \times D_c^p + D_c^f}\right) \qquad (8)$$

The selectivity of a polymer membrane for component A relative to component B, $\alpha_{A/B}$, is determined by the concentration of components in feed and permeate, which in light of eq. (9) may be written as the product of the solubility selectivity and the diffusivity selectivity.

$$\alpha_{A/B} = \frac{c_{Ap}}{c_{Bp}} \div \frac{c_{Af}}{c_{Bf}} = \frac{NPR_A}{NPR_B} \div \frac{c_{Af}}{c_{Bf}} = \frac{C_A}{C_B} \times \frac{D_A}{D_B} \div \frac{c_{Af}}{c_{Bf}}$$
$$= \left(\frac{C_A}{C_B} \div \frac{c_{Af}}{c_{Bf}}\right) \times \left(\frac{D_A}{D_B}\right) = S_S \times S_D \qquad (9)$$

where c_{if}, c_{ip} represent the concentration of component i (A or B) in the feed and permeate, respectively, (wt %), $S_S = \dfrac{C_A}{C_B} \div \dfrac{c_{Af}}{c_{Bf}}$ is the solubility selectivity and $S_D = \dfrac{D_A}{D_B}$ is the diffusivity selectivity.

EXPERIMENTAL

Materials

Poly (dimethylsiloxane) (PDMS) prepolymer was purchased from BEIJING HUAER CO., Ltd, and *tert*-butylcalix[4]arene (CA) from NANKAI UNIVERSITY. All the other solvents and reagents obtained from commercial sources were of analytical grade and used as received.

Membrane preparation

The mean diameter of CA particle is 25 μm, measured by particle size analyser (MALVERN. Ltd, mastersizer 2000) and the BET surface area is 4 m^2/g. The CA-filled PDMS membranes were prepared by solution-casting mixtures of CA particles and PDMS/toluene solutions. The casting solutions were stirred for 10 min and then poured on a flat. The PDMS were crosslinked by TEOS in the toluene solution at room temperature under the catalytic action of dibutyltin dilaurate. Twenty-four hours later, the CA-filled PDMS membranes formed as toluene evaporated completely. All the membranes were further dried in vacuum for 24 h and swelled in the feed solutions for more than 24 h before they were evaluated.

Pervaporation experiments

A schematic diagram of the pervaporation test unit is shown in Figure 1. An aqueous solution of benzene was used as the feed solution. It flows from the feed tank by the circulation pump and passes the pervaporation cell continuously. The permeate was collected by a cold trap, which was dipped into liquid nitrogen. In our pervaporation experiment, the air-side surface of all the CA-filled PDMS membranes faced the feed side of the pervaporation cell, and the effective membrane area was 25.6×10^{-4} m^2. The compositions of the feed and the permeate were analyzed by a gas chromatograph (HEWLETTPACKARD, 6890) equipped with a flame ionization detector (FID) and a PEG20,000-filled column heated to 100°C. The separation factor of benzene/water mixture was specifically expressed as eq. (10) according to eq. (9)

$$\alpha = \frac{c_{bp}}{c_{wp}} \div \frac{c_{bf}}{c_{wf}} \qquad (10)$$

where c_{bp}, c_{wp} represent the concentration of benzene and water in the permeate (wt %), respectively, c_{bf}, c_{wf} represent the concentration of benzene and water in the feed (wt %), respectively. The normalized permeation rate of benzene (NPR_b) during pervaporation was determined from eq. (11)

TABLE I
Comparison of the Pervaporation Performance of Different Membranes for the Removal of Benzene from Dilute Aqueous Solution

Membrane material	Separation factor	Benzene flux (g/m^2 h)	*NPR* (10^{-6} kgm/m^2 h)	Resource
PVDF	1100	43	—	322
Cross-linked PDMS	2886	70.9	1.96	18
PFA-*g*-PDMS	4600	—	6.5	332
PMMA-*g*-PDMS	3700	—	3.6	33
PEMA-*g*-PDMS	2400	—	2.8	7
CA-*f*-PDMS-*g*-PMMA	1800	—	7	29
CA-*f*-PDMS-*b*-PMMA	2300	—	13	25
Silicone rubber composite membrane	629	75	—	31
PDMS	3275	129	30.79	This work
CA-*f*-PDMS	5604	116	26.93	This work

$$NPR_b = (l \times W_{bp})/(t \times S) \tag{11}$$

where l is the thickness of the membrane, W_{bp} is the weight of benzene in permeate, t is the permeation time, and S is the effective membrane area.

Contact angle measurement

Contact angles for benzene and water on the surfaces of the membranes with different CA content were measured by a contact angle meter (Powereach., JC2000A) at room temperature.

Degree of swelling

The CA-filled PDMS membranes were completely dried under a reduced pressure at room temperature. The dried membranes were weighed and immersed into feed solution, pure benzene, and distilled water in sealed conical flasks, respectively. After the equilibrium reached at room temperature, the membranes were taken out of the flasks, wiped quickly with filter paper, and weighed. The degree of swelling (D_S) of the membranes is determined from eq. (12)

$$D_S = (W_s - W_d)/W_d \tag{12}$$

where W_s is the weight of the swollen membrane and W_d is the weight of the dried membrane.

Distribution of CA

The distribution of CA in the membranes was observed by polarizing microscopy (NIKON, E600).

Density

The density of the membranes, ρ_m, was obtained by weighing the samples of known area and thickness, using electronic analytical balance (OHAUS Corp, Adventure). To determine the density of CA (ρ_{CA}), a certain weight of CA was dipped into a certain weight of ethanol and the total volume was measured at 20°C.Then CA density is determined by eq. (13).

$$\rho_{CA} = \frac{W_{CA}}{V_t - \dfrac{W_{et}}{\rho_{et}}} \tag{13}$$

where W_{CA},W_{et} represent the weight of CA and ethanol, respectively, V_t is the total volume, ρ_{et} is the density of ethanol at 20°C (0.79 g/cm^3). The mean value of ρ_{CA} from this three times reproducible measurement is 1.22 g/cm^3 and the relative errors are within 3%.

Crosslinking density

The crosslinking density ρ_{Ct} of the membranes with different CA content can be calculated from Elastic modulus (E') using eq. (14), according to Uragami et al.[18]

$$\rho_{Ct} = \frac{E'}{3\rho_m \phi RT} \tag{14}$$

where E' was determined by a dynamic mechanical analyzer (PerkinElmer, Pyris Diamond) under the following conditions: frequency, 1, 2, 5, and 10 Hz; temperature, 60°C; ρ_m, the membrane density; Φ, the front factor (where $\Phi = 1$); R, the gas constant; and T, the absolute temperature.

XRD measurement

X-ray diffraction (XRD) experiments were carried out using Rigaku D/max2500 diffractometer in the scan range of 3–35° (CuKα, 40 kV/100 mA).

RESULTS AND DISCUSSION

Pervaporation performance of the filled membranes

Table I shows the typical results of our work and literature work. The membranes in our work show higher pervaporation performance for the removal of benzene from dilute aqueous solution.

Effects of CA content on the pervaporation performance

The effects of CA content (the weight ratio of CA to PDMS) on the separation factor and NPR_b are shown in Figure 2. The feed temperature is 333 K and the benzene concentration in the feed is 0.14 wt %. As is shown, there exists a valley value at 1 wt % CA content and a peak value at 3 wt % CA content in Figure 2(a,b), and in all cases, NPR_b of the control membrane (unfilled membrane) is higher than that of the filled membranes. To explain this unusual phenomenon, a series of experimental investigation is carried out.

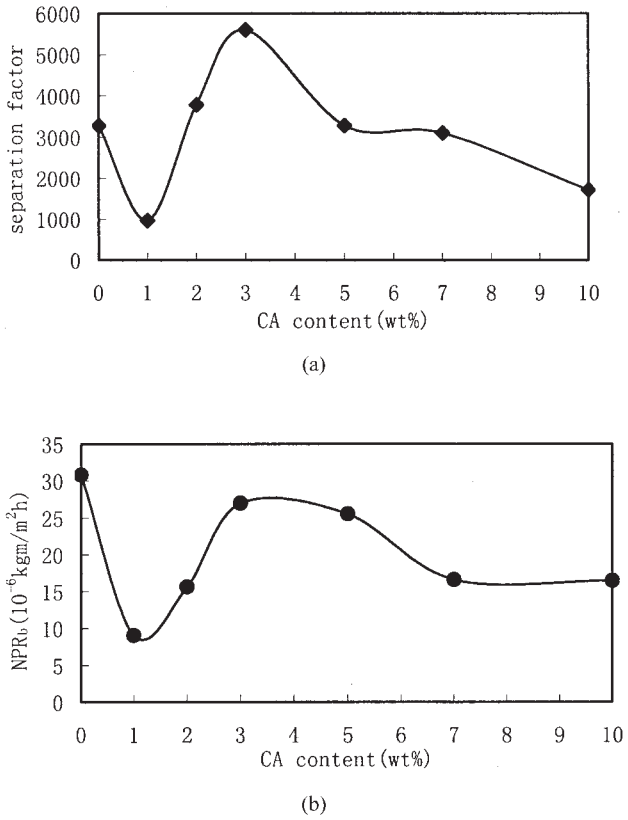

Figure 2 (a) Effect of the CA content on the separation factor. Temperature, 333 K; benzene concentration in feed, 0.14 wt%; and downstream pressure, 1.3 kPa. (b) Effect of the CA content on the normalized permeation rate of benzene. Temperature, 333 K; benzene concentration in feed, 0.14 wt%; and downstream pressure 1.3 kPa.

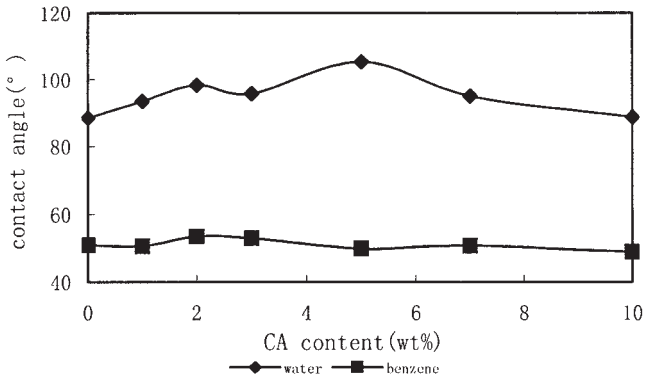

Figure 3 Effects of the CA content on the content angle for water and benzene on the membranes.

Permselectivity of CA-filled membranes

Contact angle measurement is a traditional method to describe the hydrophobicity of a dense membrane. The contact angle made by a liquid droplet deposited onto the surface of a smooth solid will have a value higher than 90° if there is low affinity between liquid and solid, and lower than 90° in case of high affinity between liquid and solid. The effect of CA content on the contact angle for water and benzene on the unfilled and filled membranes is shown in Figure 3. CA content has little effect on the contact angle for benzene; however, the contact angle for water had a maximum value at the 5 wt % CA content.

The experimental result of membrane swelling in the distilled water, feed solution, and pure benzene is shown in Figure 4(a–c). Since D_S in the distilled water is negligibly small (<0.005), the swelling in the feed solution is mainly ascribed to the adsorptive dissolution of benzene. In the feed solution, the PDMS molecule chains extend slightly so that the adsorption of benzene on CA particles can be reflected by the increase of D_S. This result proves that the addition of CA can enhance the dissolution of benzene into the membrane. On the other hand, D_S in pure benzene is extremely high (>1.6) and fluctuates with the CA content [shown in Fig. 5(c)]. This may be caused by the following three factors: (1) the serious extension of PDMS molecule chains can accommodate larger amount of benzene, (2) the adsorption character of CA will promote the swelling degree, and (3) the effect of CA as physical crosslinker will prevent the swelling degree.

Since the concentration of water in the feed solution is nearly 100% (99.86 wt %), the water concentration in the membranes swelled in feed solution can be replaced by the water concentration in the membranes swelled in distilled water. The benzene concentration in the membrane swelled in feed solution (C_b) and the S_S of the membrane can be obtained according to swelling experimental results, as shown in Figure 5

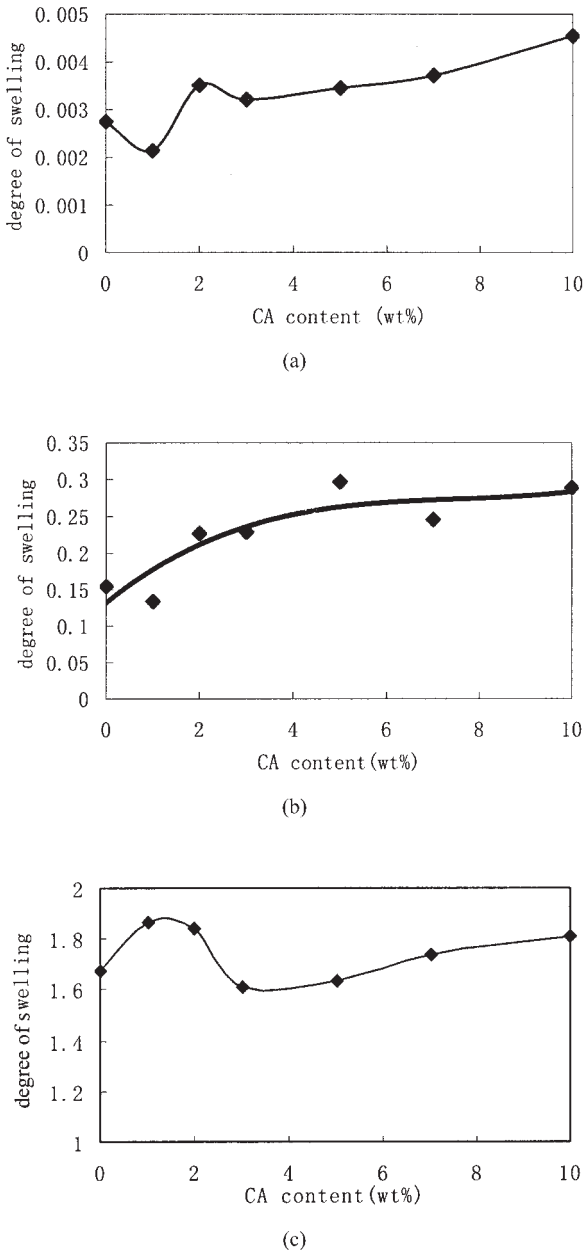

Figure 4 (a) Effects of CA content on the degree of swelling in the distilled water. (b) Effects of CA content on the degree of swelling in the feed solution. (c) Effects of CA content on the degree of swelling in pure benzene.

and Figure 6. The increase of C_b by the incorporation of CA is remarkable in Figure 6, and the experimental data is fitted by eq. (15).

$$C_b = -1.4476 \times C_{CA}^2 + 23.417 \times C_{CA} + 114.9 \quad (15)$$

where C_{CA} represents CA content (wt %) in the membrane.

The changing trend of the S_s curve is coincidently consistent with the curve of the contact angle of water, as shown in Figure 6 and Figure 3.

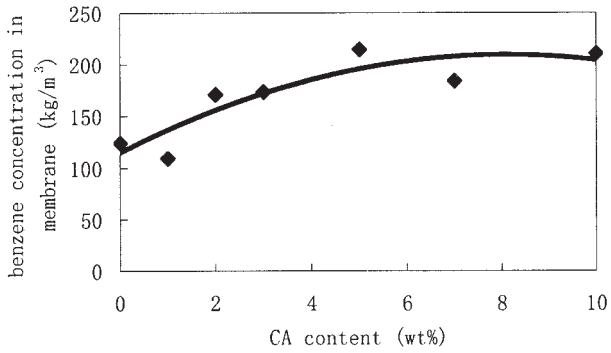

Figure 5 Effects of CA content on the benzene concentration in membrane.

Structure of CA-filled membranes

The distribution of CA particles in filled membranes with CA content 1, 2, 3, 5, 7, and 10 wt % is observed by the polarizing microscopy shown in Figure 7. The aggregated size of CA increases significantly with CA content.

For a binary polymer/filler system, the bulk density can be estimated from pure component properties if volume additivity is obeyed:

$$\rho = \frac{1}{\frac{1 - W_{CA}}{\rho_p} + \frac{W_{CA}}{\rho_{CA}}} \quad (16)$$

where W_{CA} represents weight fraction of CA, ρ_p and ρ_{CA} represent the density of PDMS and CA, respectively. As is shown in Figure 8, the experimental membrane density is consistent with eq. (16) perfectly within experimental uncertainty, which indicates that volume additivity works very well in CA-filled PDMS membranes.

In Figure 9, the elastic modulus, E′, of the membranes is shown as a function of the CA content. These E′ values can be applied to estimate the crosslinking density of the membranes by eq. (14), and subsequently the effect of CA content on the crosslinking

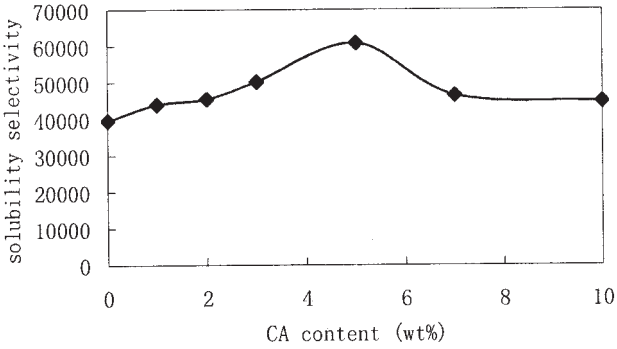

Figure 6 Effect of CA content on the solubility selectivity.

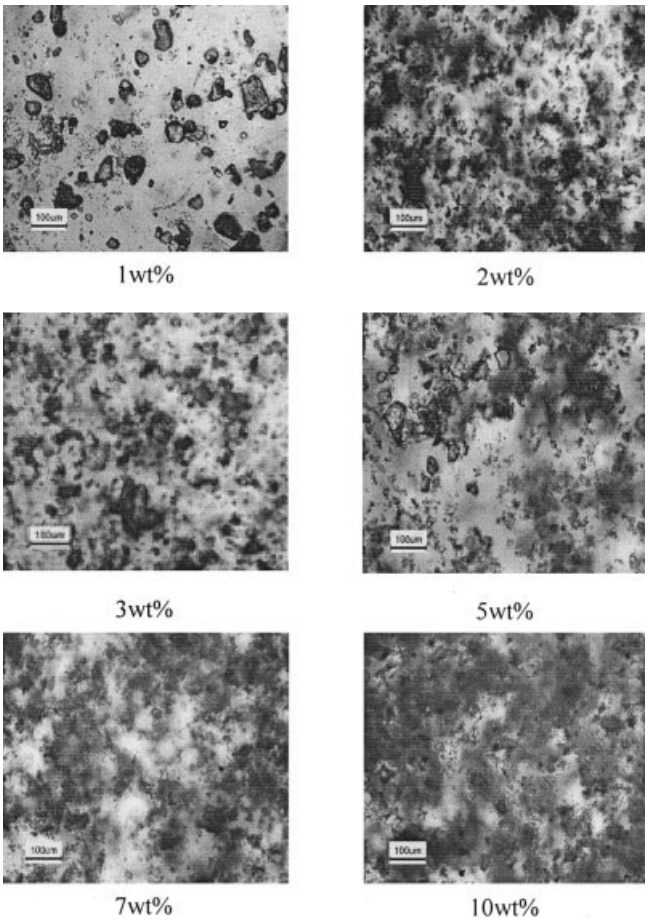

Figure 7 Polarizing micrographs of the membranes with different CA content.

density of the membranes is plotted in Figure 10. Both the elastic modulus and crosslinking density of the membranes increase with the CA content, which proves that CA particles also act as reinforcing agent and physical crosslinker for the membranes.

It has been mentioned by Uragami et al.[29] that increasing the membrane density often causes a lower

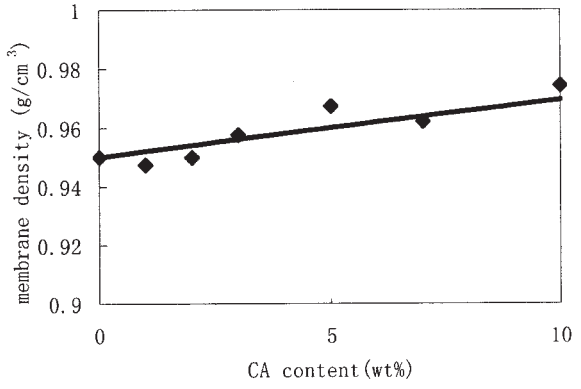

Figure 8 Effects of CA content on the membrane density. The line is the predicted density calculated from eq. (16).

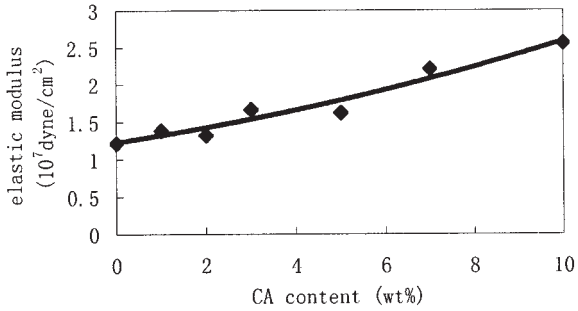

Figure 9. Effect of CA content on the elastic modulus.

NPR due to a lowered diffusivity of the components in the high-density matrix. Barrer and Skirrow[30] have reported that *NPR* decreases linearly with an increase in crosslinking density of membrane. According to the results of the membrane density and crosslinking density earlier, NPR_b should decrease monotonously with the increase of CA content. Obviously, this is contradictory with our experimental results. Our attention is thus switched to the investigation of the degree of crystallization (D_c) of the membranes.

D_c can be estimated by the ratio of crystalline area to total area in the XRD patterns. Figure 11 shows the XRD patterns of the controlled membrane (with 0 wt % CA content) and membranes with different CA content (1 ~ 10 wt %). The XRD pattern of the controlled membrane shows only a broad peak between 10°and 15°, which represents the diffraction of the minicrystal of PDMS. All the XRD patterns of the membranes with different CA contents (1 ~ 10 wt %) show crystalline peaks with different intensity. The CA crystal area, minicrystal area, total area, and the calculated D_c^p and $D_c^f$of each membrane is listed in Table II.

It is interesting to notice that the membrane with 1 wt % CA content shows much higher D_c^f than the other filled membranes with higher CA content, whereas the membrane with 3 wt % CA content shows the

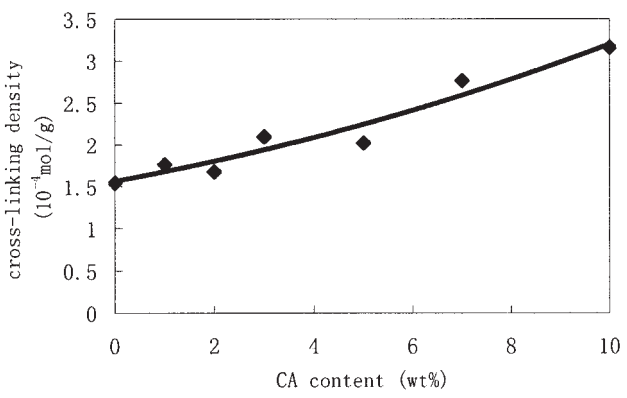

Figure 10. Effect of CA content on the crosslinked density.

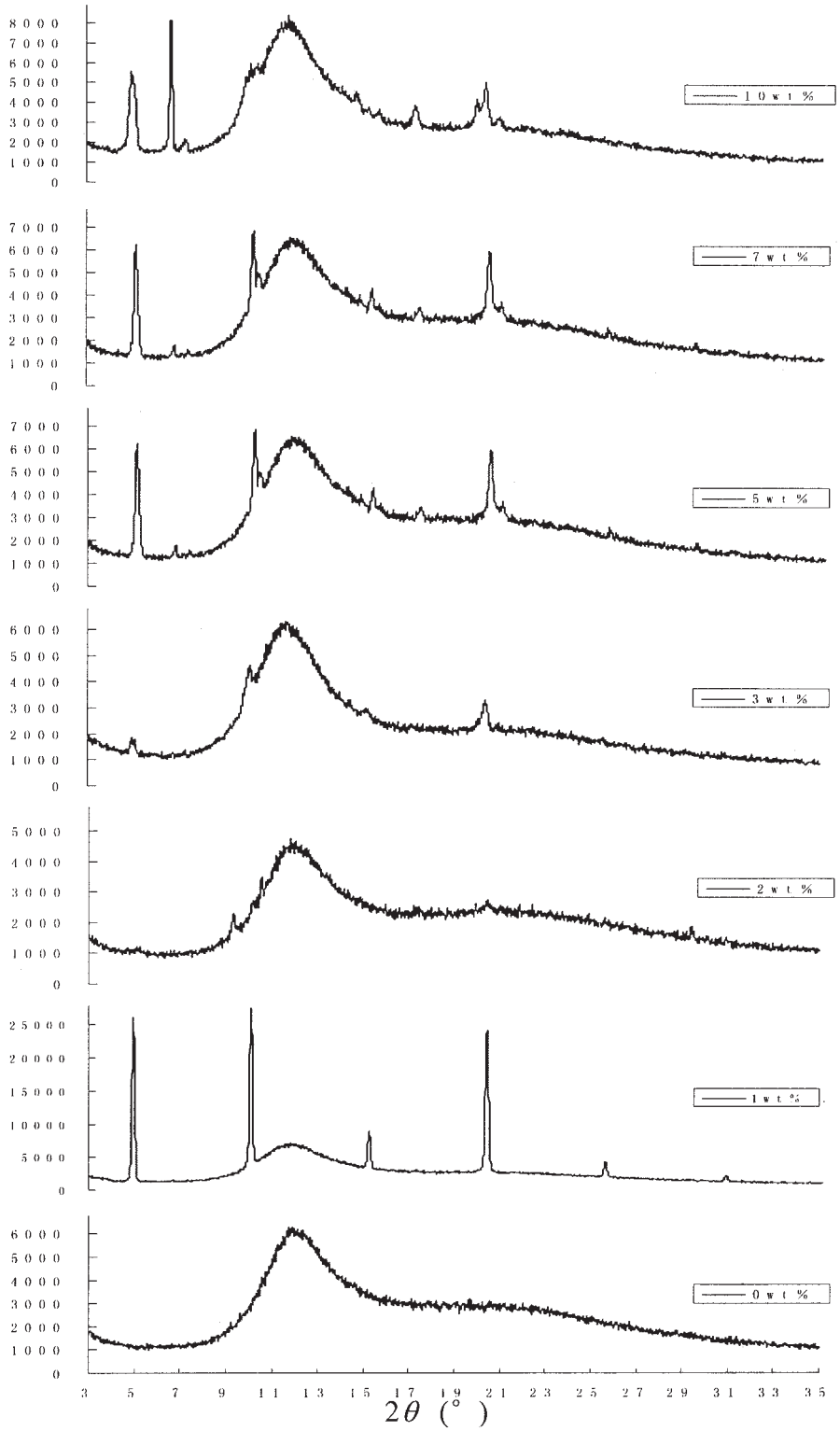

Figure 11 XRD pattern of different membranes.

minimum D_c^f. Because of the existence of amorphous part in the PDMS, the diffraction peak becomes broader, and the crystalline area of PDMS in the XRD patterns is thus overestimated. To eliminate this effect, the correction factor γ is introduced, and the fitting value of γ is 0.3308 according to our experimental data and eq. (8). The correlation coefficient R^2 is 0.9473.

On the other hand, the curve of separation factor [Fig. 2(a)] shows a valley at 1 wt % CA content with the highest D_c^f and a peak at 3 wt % CA content with

TABLE II
The CA Crystal Area, Minicrystal Area, Total Area, D_c^p and D_c^f of the Membranes with Different CA Content

CA content (wt %)	CA crystal area	Minicrystal area	Total area	D_c^p (%)	D_c^f (%)
0	0	12,000	39,000	30.77	0.00
1	16,000	14,000	50,000	28.00	32.00
2	3,400	6,500	30,000	21.67	11.33
3	3,200	13,000	35,000	37.14	9.14
5	4,900	13,000	42,000	30.95	11.67
7	6,200	8,300	32,000	25.94	19.38
10	8,900	15,000	46,000	32.61	19.35

higher S_S and lower D_c^f, which can be analyzed from two factors. Firstly, affinity of CA towards benzene from the π-rich calixarene cavity of CA can improve S_S as indicated in Figure 6. Secondly, the increase of D_c induces the decrease of S_D, which may be ascribed to the bigger molecule volume of benzene.

Effect of feed temperature

As temperature increases, polymer chains will move more freely and thus free volume in the polymer increases. The corresponding greater kinetic energies of diffusing components will result in an increase of *NPR*. Figure 12(a) shows the effects of feed temperatures on NPR_b and NPR_w of the membrane with 3 wt % CA, both NPR_b and NPR_w increase with the increase of temperature. Figure 12(b) shows an Arrhenius relationship between *NPR* and T. The activation energy for permeation can be calculated from an Arrhenius-type expression of the form

$$NPR_b = A \exp\left(-\frac{E_{a,p}}{R \times T} \right) \tag{17}$$

where A is a constant, T is the absolute temperature, $E_{a,p}$ is the activation energy for permeation, and R is the gas constant. Many researchers simply used ln (*NPR*) versus $\frac{1}{T}$ plot to calculate the activation energy. The membrane with 3 wt % CA has 11.70 and 70.58 kJ/mol activation energies for benzene and water, respectively. Activation energy of permeation shows temperature dependency of *NPR*. As the temperature increases, NPR_w increases much more rapidly than NPR_b and thus the separation factor decreases [see Fig. 12(c)].

Effect of benzene concentration in feed

From Figure 13(a), an increase of benzene concentration in feed causes a linear increase of NPR_b as also reported by other researchers.[1,2] When the benzene concentration in feed increases, the sorption of benzene in the membrane increases linearly, reflected by

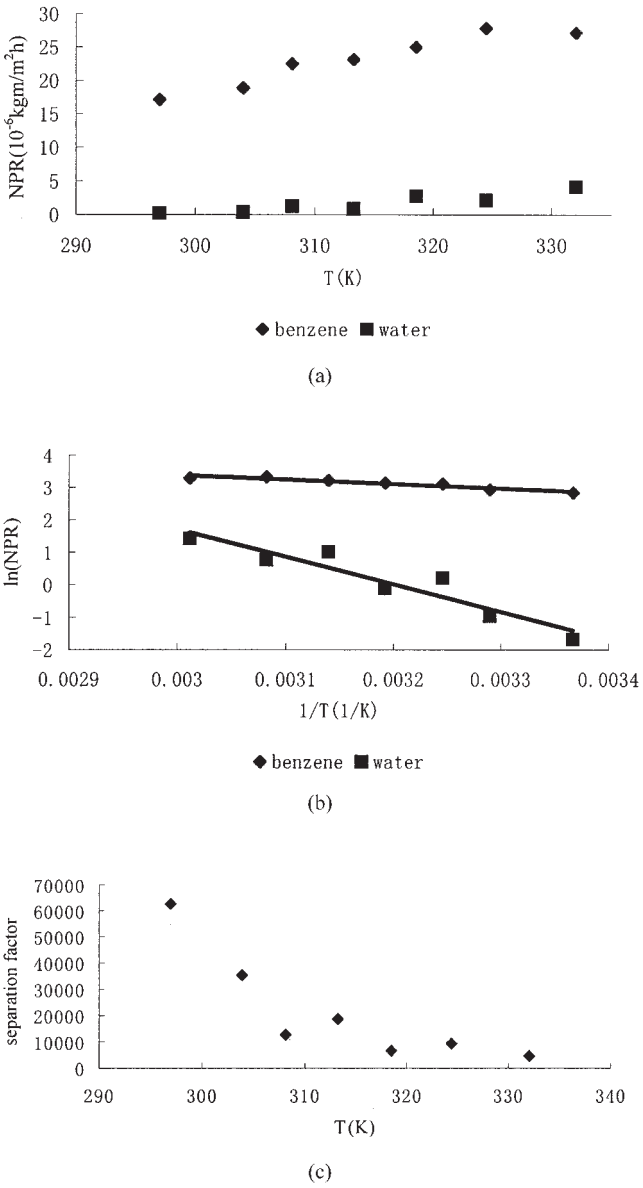

Figure 12 (a) Effect of T on NPR. Benzene concentration in feed is 0.14 wt % and downstream pressure is 1.3 kPa. (b) Relationship between 1/T and ln (*NPR*) (c) Effect of T on the separation factor. Benzene concentration in feed is 0.14 wt % and downstream pressure is 1.3 kPa.

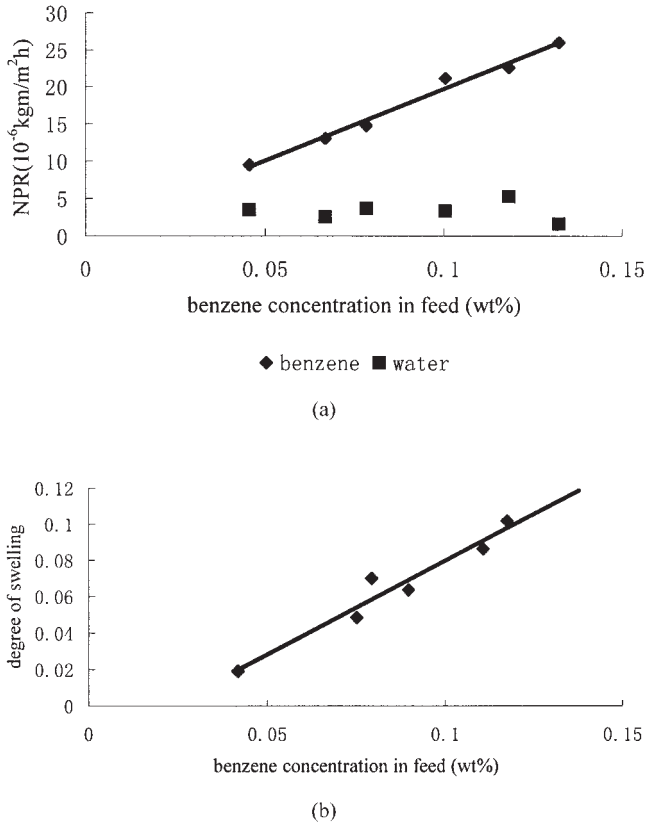

Figure 13 (a) Effect of benzene concentration in feed on *NPR*. Temperature, 333 K and downstream pressure, 1.3 kPa. (b) Effect of benzene concentration in feed on the degree of swelling.

the linear increase of D_S [see Fig. 13(b)]. Consequently, NPR_b increases because of the increase of driving force for the transport of benzene. On the other hand, NPR_w keeps almost constant as the benzene concentration increases because the benzene aqueous concentration is very dilute (less than 0.14 wt %).

Effect of the downstream pressure

When the downstream pressure increases, both NPR_b and NPR_w decrease because the pressure gradient driving force across the membrane is reduced. *NPR* of the feed component with the lower solubility in the membrane [water for the data in Fig. 14(a)] decreases more rapidly with pressure, resulting in higher separation factors [see Fig. 14(b)].

CONCLUSIONS

The membranes in this work show strong benzene permselectivity and high permeation flux. The CA content has significant effect on the permselectivity, the permeability, and the elastic modulus of the membranes. Compared with the unfilled PDMS membrane, NPR_b of the filled membranes decreases in all the cases. Among the filled membranes, the membrane with 1 wt % CA content had the highest degree of crystallization and thus the lowest NPR_b, whereas the membrane with 3 wt % CA content had the lowest degree of crystallization and thus the highest NPR_b. The decrease of NPR_b may be caused mainly by the increase of the degree of crystallization. And thus, a new model based on D_S and D_C is tentatively established to describe the mass transport in the polymer filled with crystalline adsorbent. The variation of the separation factor is mainly determined by both S_S and S_D, which are affected by the selective sorption of benzene onto the CA surface and the crystallinity of the membranes. Furthermore, the addition of CA increases the elastic modulus of membranes slightly, which indicates that CA particles also act as reinforcing agent and physical crosslinker for the membranes.

The results of this work also show that the increase of temperature and the decrease of downstream pressure can both enhance NPR_b and NPR_w, but decrease the separation factor simultaneously. As the benzene concentration in feed increases, NPR_b increases linearly but NPR_w keeps almost a constant.

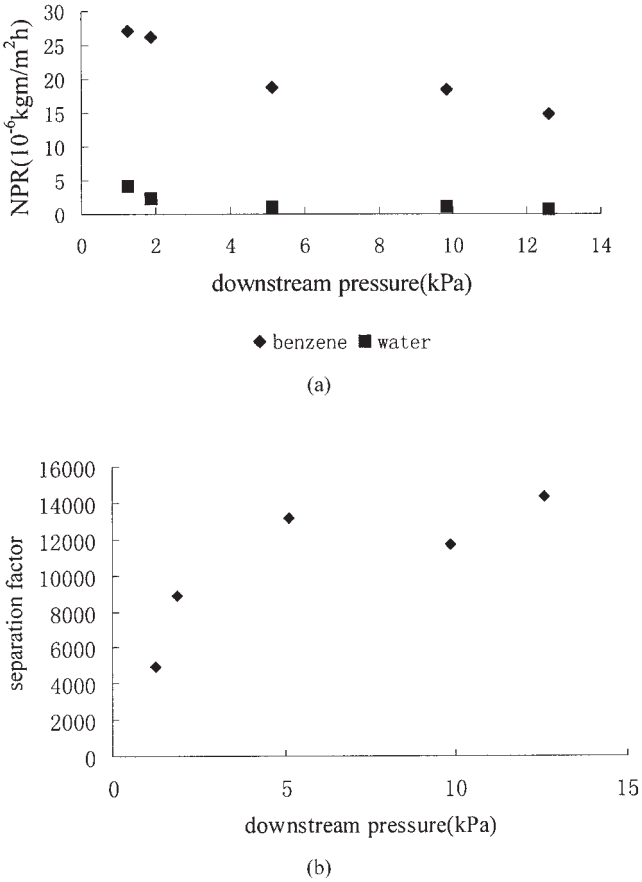

Figure 14 (a) Effect of downstream pressure on *NPR*. Temperature, 333 K and benzene concentration in feed, 0.14 wt %. (b) Effect of downstream pressure on the separation factor. Temperature, 333 K and benzene concentration in feed, 0.14 wt %.

References

1. Jian, K.; Pintauro, P. N.; Ponangi, R. J Membr Sci 1996, 117, 117.
2. Jian, K.; Pintauro, P. N. J Membr Sci 1997, 135, 41.
3. Hofmann, D.; Fritz, L.; Paul, D. J Membr Sci 1998, 144, 145.
4. Li, S.; Tuan, V. A.; Falconer, J. L.; Noble, R. D. Ind Eng Chem Res 2001, 40, 1952.
5. Hitchens, L.; Vane, L. M.; Alvarez, F. R. Separ Purif Technol 2001, 24, 67.
6. Peng, M.; Vane, L. M.; Liu, S. X. J Hazard Mater 2003, 98, 69.
7. Uragami, T.; Yamada, H.; Miyata, T. J Membr Sci 2001, 187, 255.
8. Kim, H. J.; Nah, S. S.; Min, B. R. Adv Environ Res 2002, 6, 255.
9. Abou, N. I.; Das, A.; Saraf, A.; Sirkar, K. K. J Membr Sci 1999, 158, 187.
10. Ji, W.; Hilaly, A.; Sikdar, S. K.; Hwang, S. T. J Membr Sci 1994, 97, 109.
11. Eric, F.; Quang, T. N. J Chem Tech Biotechnol 1996, 65, 221.
12. Kaddour, D. M.; Nguyen, Q. T.; Clement, R.; Germain, Y. J Membr Sci 1998, 146, 125.
13. Yeom, C. K.; Kim, H. K.; Rhim, J. W. J Appl Polym Sci 1999, 73, 601.
14. Mishima, S.; Nakagawa, T. J Appl Polym Sci 2000, 78, 1304.
15. Mishima, S.; Nakagawa, T. J Appl Polym Sci 1999, 73, 1835.
16. Hongyuan, W.; Xiao, L.; Kazuhiro, T.; Hidetoshi, K.; Ken-ichi, O. J Appl Polym Sci 1998, 36, 2247.
17. Jan, S.; Petr, S.; Vladimir, M.; Zbynek, P.; Jiri, P.; Miroslav, B. J Appl Polym Sci 1996, 61, 1333.
18. Uragami, T.; Ohshima, T.; Miyata, T. Macromolecules 2003, 36, 9430.
19. Jiwon, R.; Younkook, K. J Appl Polym Sci 2000, 75, 1699.
20. Miyata, T.; Yamada, H.; Uragami, T. Macromolecules 2001, 34, 8026.
21. Vankelecom, I. F. J.; Depre, D.; Beuketaer, S. D.; Uytterhoeven, J. B. J Phy Chem 1995, 99, 13193.
22. Jonquieres, A.; Fane, A. J Membr Sci 1997, 125, 245.
23. Li, L.; Xiao, Z. Y.; Zhang, Z. B.; Tan, S. J. Chem Eng J 2004, 97, 83.
24. Chen, X.; Ping, Z. H.; Long, Y. C. J Appl Polym Sci 1998, 67, 629.
25. Uragami, T.; Meotoiwa, T.; Miyata, T. Macromolecules 2003, 36, 2041.
26. Cecile, V.; Eric, F.; Denis, R.; Jerome, B.; Daniel, S. Ind Eng Chem Res 2001, 40, 1559.
27. Barrer, R. M.; Barrie, J. A.; Rogers, M. G. J Polym Sci Part A: Polym Chem 1963, 1, 2565.
28. Barrer, R. M.; Crank, J.; Park, G. S. Diffusion in Polymers, Academic Press: London, 1968; p 165.
29. Uragami, T.; Meotoiwa, T.; Miyata, T. Macromolecules 2001, 34, 6806.
30. Barrer, R. M.; Skirrow, G. J Polym Sci 1948, 3, 549.
31. Baker, R. W. U.S. Pat. 5,169,533 (1992).